JOURNAL OF BACTERIOLOGY, Oct. 2011, p. 5498–5509 Vol. 193, No. 19
0021-9193/11/$12.00 doi:10.1128/JB.00438-11

Glycosylation of DsbA in *Francisella tularensis* subsp. *tularensis*▽†

Rebecca M. Thomas,[1]‡ Susan M. Twine,[2]‡ Kelly M. Fulton,[2] Luc Tessier,[2] Sara L. N. Kilmury,[2] Wen Ding,[2] Nicholas Harmer,[3] Stephen L. Michell,[3] Petra C. F. Oyston,[1] Richard W. Titball,[3]* and Joann L. Prior[1]

Defence Science and Technology Laboratory, Porton Down, Salisbury, Wiltshire SP4 0JQ, United Kingdom[1]*; Proteomics Group, Institute for Biological Sciences, National Research Council Canada, 100 Sussex Drive, Ottawa, Ontario K1A 0R6, Canada*[2]*; and College of Life and Environmental Sciences, University of Exeter, Exeter EX4 4QD, United Kingdom*[3]

Received 31 March 2011/Accepted 20 July 2011

In *Francisella tularensis* subsp. *tularensis*, DsbA has been shown to be an essential virulence factor and has been observed to migrate to multiple protein spots on two-dimensional electrophoresis gels. In this work, we show that the protein is modified with a 1,156-Da glycan moiety in *O*-linkage. The results of mass spectrometry studies suggest that the glycan is a hexasaccharide, comprised of *N*-acetylhexosamines, hexoses, and an unknown monosaccharide. Disruption of two genes within the *FTT0789-FTT0800* putative polysaccharide locus, including a *galE* homologue (*FTT0791*) and a putative glycosyltransferase (*FTT0798*), resulted in loss of glycan modification of DsbA. The *F. tularensis* subsp. *tularensis* Δ*FTT0798* and Δ*FTT0791*::Cm mutants remained virulent in the murine model of subcutaneous tularemia. This indicates that glycosylation of DsbA does not play a major role in virulence under these conditions. This is the first report of the detailed characterization of the DsbA glycan and putative role of the *FTT0789-FTT0800* gene cluster in glycan biosynthesis.

Glycosylation is one of the most common modifications of eukaryotic proteins and has been estimated to occur in up to half of all eukaryotic gene products (2). Whereas eukaryotic glycoproteins have long been the focus of extensive research, the accepted dogma was that prokaryotes could not glycosylate their proteins, and it is only relatively recently that this view has changed (31, 33, 46). The first reports of prokaryotic protein glycosylation focused upon the S-layer glycoproteins of the *Archaea* domain (32), and there has been an increase in the number of studies reporting the characterization of prokaryotic glycoproteins. To date, such proteins have been primarily surface associated or secreted and modified with a diverse array of glycan moieties (6, 7, 22, 42–45, 48, 52, 58, 61, 62). For some pathogens such as *Campylobacter jejuni* (19) and *Clostridium difficile* (57), protein glycosylation is important for the function and assembly of flagellins. For other pathogens such as *Neisseria gonorrhoeae*, glycoproteins are important for adherence of the bacteria to the host cells (4, 10, 50). Glycosylation can also play a role in the interaction of the pathogen with the immune system of the host. For example, complement-mediated lysis is blocked by antibodies directed against the 1,3 galactose modification of pili in *Neisseria meningitidis* (21).

Francisella tularensis is the causative agent of tularemia, a disease that affects many mammals, including humans and rodents. The bacterium is a small, 0.2- to 0.5-μm by 0.7- to 1.0-μm, Gram-negative intracellular pathogen, and the natural reservoir is thought to be rodents with ticks being the primary vector (14). *F. tularensis* is divided into three subspecies, *tularensis*, *holarctica*, and *mediasiatica*. Despite being genetically closely related to *F. tularensis*, *Francisella novicida* currently retains its own species designation. *F. tularensis* subsp. *tularensis* is the most virulent subspecies, and it is highly pathogenic for humans. *F. novicida* is considered less virulent in humans with some reports of infections in immunocompromised individuals. The pathogen has received much attention in recent years due to concerns regarding its potential use as a biowarfare agent. Despite intensive efforts to increase understanding of this highly virulent pathogen, a detailed knowledge of the mechanisms of virulence is still lacking.

Recent work has begun to identify and characterize glycoproteins expressed by *Francisella*. The *F. tularensis* subsp. *tularensis* PilA protein has been shown to migrate to an apparent molecular mass 4 to 5 kDa larger than the predicted molecular mass of 14.6 kDa (16). In contrast, when the *Francisella pilA* gene was expressed in a glycosylation-defective strain of *Pseudomonas aeruginosa*, the *Francisella* PilA protein migrated with an apparent molecular mass of 14 kDa. A subsequent study reported that *Francisella* PilA proteins undergo *O*-linked glycosylation when expressed in *N. gonorrhoeae* (41).

A recent study by Balonova et al. (3) used several approaches such as gel-based carbohydrate staining and lectin blotting to identify modified glycoproteins in *F. tularensis* subsp. *holarctica*. Both the PilA protein and the DsbA homologous protein FTH1071 were identified as putative glycoproteins. However, the type and linkage of the putative glycan moieties were not determined. Both PilA and DsbA are associated with virulence (16, 37). However, the nature and role of any potential modifying glycans remain unknown.

* Corresponding author. Mailing address: Geoffrey Pope Building, School of Biosciences, College of Life and Environmental Sciences, University of Exeter, Stocker Road, Exeter EX4 4QD, United Kingdom. Phone: 44 (0) 1392 725157. Fax: 44 (0) 1392 723434. E-mail: R.W.Titball@exeter.ac.uk.

† Supplemental material for this article may be found at http://jb.asm.org/.

‡ These authors contributed equally to this work.

▽ Published ahead of print on 29 July 2011.

An analysis of the genome of *F. tularensis* subsp. *tularensis* strain SchuS4 reveals two potential polysaccharide biosynthesis gene clusters. The first cluster is associated with the biosynthesis of O antigen. The O antigen is a virulence determinant and a protective antigen (36). The product of the second polysaccharide biosynthesis gene cluster (*FTT0789-FTT0800*) (Table 1) is unknown (30). In *F. novicida* and the *F. tularensis* subsp. *holarctica* LVS (LVS for live vaccine strain), homologues of some of these genes have been identified as playing a role in virulence (28, 65).

To date, there have been no reports of the structures of the *Francisella* glycoprotein glycans or the genes involved with the glycan biosynthesis. The aims of this study were to determine whether *F. tularensis* subsp. *tularensis* has a protein glycosylation system, what the structure and linkage of the glycan are, and which genes or gene clusters are involved in the biosynthesis of the glycan. In addition, we sought to investigate the role of the DsbA glycan in virulence in the *F. tularensis* murine model of subcutaneous tularemia.

MATERIALS AND METHODS

Bacteria, plasmids, growth conditions, and general enzymes and chemicals. The bacterial strains and plasmids used in this study are listed in Table S1 in the supplemental material. Unless otherwise stated, enzymes for the manipulation of DNA and nucleotides were obtained from Roche Diagnostics Limited (Lewes, United Kingdom); chemicals were obtained from Sigma Chemical Co. (Poole, United Kingdom), and culture medium was obtained from Oxoid Limited (Basingstoke, United Kingdom).

F. tularensis subsp. *tularensis* strains (23, 30) were cultured on blood cysteine glucose agar (BCGA) supplemented with 10 ml of 10% (wt/vol) histidine per liter or on modified Thayer Martin agar (TM) (BBL Gc agar base [Becton Dickinson, United Kingdom] supplemented with 1% [wt/vol] hemoglobin and 1% [vol/vol] BBL IsoVitaleX [Becton Dickinson]) or in liquid culture in Chamberlain's defined medium (CDM) (8). *Escherichia coli* was cultured on Luria-Bertani (LB) plates or broth (5). Chloramphenicol (Cm) was added to growth media at 25 μg/ml for *E. coli* and 10 μg/ml for *F. novicida* and *F. tularensis* subsp. *tularensis*. Kanamycin (Kan) was added to growth media at 25 μg/ml for *E. coli* and 5 μg/ml for *F. tularensis* subsp. *tularensis.*

Construction of the *FTT0791* and *FTT0798* disruption cassettes. *FTT0791* was targeted for deletion and insertion of a Cm resistance cassette. It was anticipated that this mutation would disrupt the function of the cluster. The use of chloramphenicol as a marker has been approved for this specific study in the United Kingdom by a genetic manipulation safety committee and by our national health and safety authorities. An internal region of genes *rpe* and *galE* (the upstream region) and an internal region of genes *FTT0791* and *FTT0793* (the downstream region) were amplified by the PCR using primers GalE LF and GalE LR and GalE RF and GalE RR. The disruption cassette was then constructed by a splicing by overhang extension PCR (9) using a PCR-amplified Cm acetyltransferase gene (*cat*) using primers Cm F and Cm R. The 4.6-kb DNA fragment was ligated into SalI-digested pSMP22 and transformed into *E. coli* S17-λ pir (47). The resultant plasmid was designated pSMP22::Δ*FTT0791.* Oligonucleotides used in this study are detailed in Table S2 in the supplemental material.

Another gene in the *FTT0789-FTT0800* cluster, *FTT0798*, was also targeted for mutation. For the upstream region, an internal region of *FTT0797* to the start codon of *FTT0798* was amplified by the PCR using primers *FTT0798* LF and *FTT0798* LR. A BamHI site was incorporated onto the 3′ end to aid cloning. For the downstream region, the *FTT0798* stop codon through to an internal site in *FTT0799* was amplified with a BamHI site being incorporated into the 5′ end to aid cloning using primers *FTT0798* RF and *FTT0798* RR. The upstream and downstream fragments were each cloned into pGEM-T Easy (Promega, Southampton, United Kingdom). The flanks were excised from pGEM-T Easy with MluI and BamHI and ligated together into MluI-digested pSMP75 (see Table S2 in the supplemental material) to produce pSMP75::Δ*FTT0798*.

Conjugal transfer of pSMP22::Δ*FTT0791*. pSMP22::Δ*FTT0791* was introduced into *F. tularensis* subsp. *tularensis* by conjugation by the method of Golovliov et al. (17). Conjugation mixtures were incubated on BCGA plates at 25°C for 12 h before selection of transconjugants. The transconjugants were selected on modified Thayer Martin plates containing 100 μg/ml polymyxin B and 10 μg/ml Cm. The plates were incubated at 37°C for up to 5 days.

Cryotransformation of pSMP75::Δ*FTT0798*. pSMP75::Δ*FTT0798* was cryotransformed into *F. tularensis* subsp. *tularensis* by the method of Quarry et al. (38). Cryotransformants were recovered on BCGA plates for 4 h at 37°C and plated onto TM plates supplemented with 10 μg/ml kanamycin to select for merodiploids. Subsequent resolution of merodiploids was done on TM plates containing 5% (wt/vol) sucrose.

Analysis of transconjugants and cryotransformants. Southern blotting, DNA sequencing, and PCR were used to confirm the deletion in the *FTT0791* gene and the *FTT0798* gene regions using primers GalE probe F and GalE probe R or *FTT0798* LR and *FTT0798* screen F and GalE F and Cam R or GalEF and GalER. The *F. tularensis* subsp. *tularensis galE* and *FTT0798* mutants were designated Δ*FTT0791*::Cm and Δ*FTT0798*, respectively (see Fig. S1 in the supplemental material).

RT-PCR. To determine the effects of mutations on the expression of adjacent genes, reverse transcription PCR (RT-PCR) was carried out. Bacteria were cultured in modified cysteine partial hydrolysate broth (MCPH) at 37°C with shaking at 180 rpm until the cells were growing exponentially. RNA extraction was performed using an RNeasy minipreparation kit (Qiagen). Contaminating DNA was removed using Turbo DNA-*free* (Ambion), and mRNA was reverse transcribed using Superscript III reverse transcriptase (Invitrogen). RT-PCRs without reverse transcriptase were used as controls for the gene-specific PCRs. Gene-specific primers were used to confirm the presence or absence of the transcript in the strains used (see Fig. S2 in the supplemental material).

Two-dimensional polyacrylamide gel electrophoresis (2D-PAGE) analysis of *F. tularensis* subsp. *tularensis*. For all strains, bacteria were grown on BCGA plates at 37°C. Two plates were harvested for each strain. Whole-cell protein preparations were made by resuspending the cell pellet in lysis buffer {7 M urea, 2 M thiourea, 4% 3-[(3-cholamidopropyl)-dimethylammonio]-1-propanesulfonate (CHAPS), 1% dithiothreitol (DTT), 0.5% amidosulfobetaine-14 (ASB-14)} (54) and shaken at room temperature for 1 h or sonicated until clear. The cell lysates were centrifuged for 10 min at 12,000 × *g*, and the proteins were precipitated from supernatants with 10 volumes of ice-cold acetone. The proteins were pelleted by centrifugation, and the pellets were air dried before being resuspended in lysis buffer.

Quantified cell lysates were diluted in protein solubilization buffer containing 7 M urea, 2 M thiourea, 4% CHAPS, 1% DTT, and 0.5% ASB-14, 0.5% (vol/vol) pH 3 to 10 Biolytes, and 0.003% Orange G (Bio-Rad, Hercules, CA). For wild-type and mutant strains, the extracted proteins (100 μg) were separated using immobilized pH gradient strips (IPG) (linear gradient from pH 4 to 7) (17 cm) (Bio-Rad, Hercules, CA). The proteins were loaded onto the IPG strips by in-gel rehydration overnight. Isoelectric focusing (IEF) was conducted using a Protein IEF Cell (Bio-Rad, Hercules, CA). Briefly, the running conditions were as follows: 200 V for 1 h, 500 V for 1 h, 6-h ramp to 5,000 V, hold at 5,000 V for a total of 80,000 to 100,000 V h. These conditions were the conditions routinely used within the laboratory and were optimized for this IEF cell for focusing of 100 to 400 μg protein. Following IEF, the IPG strips were equilibrated for 25 min in equilibration buffer containing 2% SDS, 50 mM Tris-HCl (pH 8.8), 6 M urea, 30% glycerol, and 1% DTT. This was immediately followed by a second 25-min equilibration strip in the same solution containing 4% iodoacetamide in the place of DTT. The IPG strips were then rinsed in SDS gel running buffer (Bio-Rad, Hercules, CA) and embedded in a 12% homogeneous polyacrylamide gels (190 by 190 by 1.5 mm) with 1% agarose overlay with bromophenol blue (Bio-Rad, Hercules, CA). Gels (1% acrylamide) were run using PowerPac 1000 (Bio-Rad, Hercules, CA) at 24 mA for 5 h with the temperature during electrophoresis maintained at 20°C by water cooling. The gels were stained sequentially with Emerald Q glycostain (Invitrogen, Carlsbad, CA) and Sypro Ruby protein stain (Bio-Rad, Woodbridge, Ontario, Canada). Images of gels were collected using FluorS (Bio-Rad, Hercules, CA).

Protein spots were excised and digested with trypsin or endoproteinase Asp-N, as described previously (54). The resulting peptides were analyzed by nanoliquid chromatography coupled to tandem MS (nLC-MS/MS) using electrospray ionization (ESI) as the ion source as recently described (56, 57). The peak list files of MS/MS spectra of the excised protein spots were searched against the NCBI *F. tularensis* database (5 May 2007) with 12,283 entries using the MASCOT search engine (version 2.2.0) (Matrix Science, London, United Kingdom) or PEAKS studio (Bioinformatics Solutions Inc., Waterloo, Ontario, Canada) for protein identification. The mass tolerance for precursor ions is ±1.0 Da, and the mass tolerance for fragment ions is ±1.0 Da with trypsin or Asp-N. Ion scores of 30 and above indicated identity. In addition, all spectral matches were verified manually. Unmatched MS/MS spectra were examined manually to determine the sequences of peptide y and b type ions.

TABLE 1. Homologues of *FTT0789-FTT0800* cluster proteins

Protein	Predicted function	Conserved domain(s)	Nearest homologue[a]	No. of identical or similar residues (*n*)[b]	Homologue in *F. tularensis* subsp. *holarctica*	Homologue in *F. novicida*
FTT0789 (Rpe)	D-Ribulose-phosphate 3-epimerase	Ribulose-5-phosphate 3-epimerase	Ribulose-phosphate 3-epimerase [*Vibrio fischeri* ES114] (YP_205671.1)	148 identical and 172 similar (222)	D-Ribulose-phosphate 3-epimerase (YP_514087.1)	D-Ribulose-phosphate 3-epimerase (YP_898856.1)
FTT0790	Sugar transferase family protein	Bacterial sugar transferase	Bacterial sugar transferase family protein [*Anaerobaculum hydrogeniformans* ATCC BAA-1850] (ZP_06439449)	146 identical and 227 similar (385)	Sugar transferase family protein (YP_514086.1)	Sugar transferase involved in lipopolysaccharide synthesis (YP_898855.1)
FTT0791 (GalE)	UDP-glucose 4-epimerase	UDP-glucose-4-epimerase	UDP-glucose 4-epimerase [*Bacillus subtilis* subsp. *subtilis* strain 168] (ZP_03593702)	207 identical and 246 similar (327)	Glycosyltransferases group 1 family protein (YP_514084.1)	Glycosyltransferase, group 1 (YP_898853.1)
FTT0792	Glycosyltransferase	GT1_like_4, RfaG	Glycosyltransferase WbpZ [*Yersinia rohdei* ATCC 43380] (ZP_04611468)	171 identical and 255 similar (407)	Glycosyltransferase group 1 family protein (YP_514084)	Glycosyltransferase, group 1 (YP_898853)
FTT0793	ABC transporter, ATP-binding protein, and membrane protein	d03251, ABCC_MsbA	ATPase [*Roseburia intestinalis* L1-82] (ZP_04742579)	199 identical and 332 similar (577)	ABC transporter, ATP-binding protein, and membrane protein (YP_514083.1)	ABC transporter, ATP-binding protein (YP_898852.1)
FTT0794	Hypothetical protein	Bifunctional protein cd02523, PC_cytidylyltransferase	Phosphoserine phosphatase, SerB [*Helicobacter hepaticus* ATCC 51449] (NP_859609)	108 identical and 143 similar (195)	Hypothetical protein (FTL_1427 and YP_514082.1)	No homologue
FTT0795	Hypothetical protein	pfam08242, methyltransf_12, methyltransferase domain	Methyltransferase type 12 [*Desulfovibrio desulfuricans* subsp. *desulfuricans* strain ATCC 27774] (YP_002479604.1)	88 identical and 135 similar (185)	Hypothetical protein (FTL_1426 and YP_514081.1)	No homologue
FTT0796	Hypothetical protein	LicC superfamily pfam04991	LicD family protein [*Clostridium perfringens* C strain JGS1495] (EDS80936.1)	31 identical and 47 similar (77)	Hypothetical protein (FTL_1425 and YP_514080.1)	No homologue
FTT0797	Glycosyltransferase family protein	cd00761:Glyco_tranf_GTA_type	TagF domain-containing protein [*Enterococcus faecalis* T2] (ZP_05425945.1)	98 identical and 144 similar (227)	Glycosyltransferase family protein (YP_514079.1)	Glycosyltransferase family protein (YP_898849)
FTT0798	Glycosyltransferase family protein	cd00761:Glyco_tranf_GTA_type	TagF domain-containing protein [*Enterococcus faecalis* T2] (ZP_05425945.1)	101 identical and 174 similar (315)	Glycosyltransferase family protein (YP_514078.1)	Glycosyltransferase family protein (YP_898848.1)
FTT0799	Glycosyltransferase group 1 family protein	d03809, GT1_mtfB_like	Putative glycosyltransferase, group 1 [*Leptospirillum rubarum*] (EAY56975.1)	114 identical and 80 similar (333)	Glycosyltransferase group 1 family protein (YP_514077.1)	Glycosyltransferase group 1 family protein (YP_898847.1)
FTT0800	Haloacid halogenase-like hydolase family protein	Predicted hydrolase (HAD[c] superfamily), Pyr-5-nucleotidase, pyrimidine 5′-nucleotidase	HAD superfamily hydrolase ["*Candidatus* Pelagibacter ubique" HTCC1062] (YP_265889.1)	80 identical and 129 similar (212)	HAD family hydrolase (YP_001428940.1)	No homologue

[a] For the homologue columns, the homologue is shown first. The species is shown in brackets, and the NCBI accession number is shown in parentheses.

[b] The number of residues identical to those of *F. tularensis* SchuS4 (number of invariant residues) and the number of similar residues (number of invariant and/or conserved residues) are shown. The total number of residues (*n*) is shown in parentheses.

[c] HAD, haloacid dehalogenase.

Ion pairing normal-phase liquid chromatography (IP-NPLC) for enrichment of *Francisella tularensis* glycopeptides. Samples (100 to 200 μg) of protein from *Francisella* SchuS4 cell lysates (produced as 2D-PAGE samples) were precipitated by incubation at −20°C for 1 h in 4 volumes of ice-cold acetone and then pelleted by centrifugation. The acetone was removed, and the protein pellet was air dried in a laminar flow hood. Proteins were partially dissolved in 50 mM ammonium bicarbonate, and 2.5 to 5 μg of trypsin was added. The suspension was incubated at 37°C for 14 h, and this resulted in complete solubilization and digestion of the SchuS4 proteome.

IP-NPLC experiments were carried out using an Ettan multidimensional liquid chromatography (MDLC) system (Amersham Biosciences AB, Uppsala, Sweden) coupled to a Q-TOF2 hybrid quadrupole time of flight (Q-TOF) mass spectrometer (Waters, Milford, MA). Peptide-containing samples were dried under vacuum to 1 μl and then diluted to 10 μl with 90% acetonitrile (ACN) and 1% trifluoroacetic acid (TFA). The samples were then injected onto a polyhydroxyethyl aspartamide column (The Nest Group, Inc., Southborough, MA) equilibrated with 10% buffer B (0.1% formic acid in high-performance liquid chromatography [HPLC]-grade H_2O; the equilibration time was 7 min at 120 μl min^{-1}). Peptides were loaded with 10% buffer B at 60 μl min^{-1} for 4 min. Peptides were eluted using the following gradient: 10 to 30% buffer B over 5 min, 30 to 60% buffer B over 5 min, 60 to 98% buffer B over 2 min, and 10% buffer B for a 5-min reequilibration (120 μl min^{-1}). In this case, solvent A was ACN and 0.1% FA. A postcolumn splitter was used to direct ~400 nl min^{-1} to the ESI source to obtain MS chromatograms for each sample; the remainder of the flow was collected in 30- to 60-s fractions.

MS analysis of tryptic glycopeptides. The glycopeptide fractions (90 μl for each fraction) were collected and dried to 1 μl, which was then resuspended in 100 μl of 0.1% formic acid (aqueous) and analyzed by nanoflow reversed-phase liquid chromatography (RPLC) coupled to MS using ESI (nanoRPLC-ESI-MS) using a nanoAcquity UltraPerformance LC (UPLC) system coupled to a Q-TOF Ultima hybrid quadrupole–TOF mass spectrometer (Waters, Milford, MA) or an LTQ linear ion trap mass spectrometer. The peptides were first loaded onto a 180-μm-inner-diameter (ID) by 20-mm 5-μm symmetry C_{18} trap column (Waters, Milford, MA) and then eluted to a 100-μm-ID by 10-cm 1.7-μm BEH130C18 column (Waters, Milford, MA) using a linear gradient from 1% to 45% solvent B (ACN plus 0.1% formic acid) in 18 min, 45% to 85% solvent B for 3 min, 85% to 1% solvent B over 1 min, and hold for 8 min at 1% solvent B. Solvent A was 0.2% formic acid in water.

Determination of glycan linkage sites by ETD. Electron transfer dissociation (ETD) experiments were carried out using IP-NPLC-purified glycopeptides on an LTQ XL linear ion trap instrument (Thermo Scientific, Waltham, MA), coupled to a nanoAcquity UPLC system (Waters, Milford, MA). The peptide separation was carried out using the conditions described above. Collisional activation MS/MS was performed initially to confirm the identity of the glycopeptide. ETD MS/MS was then carried out targeting the m/z 986.6^{4+} tryptic glycopeptide ion, with fluoranthene as the anionic reagent. ETD conditions were as described previously (57), with the exception that the activation time was reduced to 70 ms.

Determination of glycan linkage sites by β-elimination. The determination of glycan linkage sites by β-elimination was carried out essentially by the method of Rademaker et al. (39). Briefly, approximately 250 pmol of IP-NPLC-separated DsbA tryptic glycopeptide T^{32} was evaporated almost to dryness before adding 300 μl of 25% ammonium hydroxide and incubating at 45°C for 10 h. The reaction was stopped by removing the NH_4OH using vacuum centrifugation, and the β-eliminated peptide was resuspended in 50% methanol and 0.1% formic acid (vol/vol). nLC-MS/MS was carried out on the β-eliminated peptides using a Q-TOF Ultima hybrid quadrupole time of flight mass spectrometer, targeting the predicted m/z of the triply charged peptide precursor ion with glycan removed (929.47^{3+}). A collision energy of 38 V was used (laboratory frame of reference). A tryptic digest of the 2D gel spot corresponding to the unmodified form of the DsbA protein was run under the same conditions as a control.

Measurement of glycan accurate masses. Accurate masses of DsbA glycan fragments were measured using an LTQ Orbitrap mass spectrometer (Thermo Scientific, Waltham, MA) by performing targeted nLC-MS/MS on the C-terminal glycopeptide ion produced either by tryptic digestion (m/z 986.6^{4+}) or Asp-N digestion (m/z $1{,}168.2^{3+}$). All spectra were acquired in Fourier transform mode (FT) at 100,000 resolution. Collision-induced dissociation (CID) at 30 V (for the quadruply protonated tryptic peptide) or 35 V (for the triply protonated Asp-N peptide) provided accurate mass measurements for the glycan oxonium ion and its larger fragment ions (m/z 1,157, 954, 792, and 630). High-energy collision-induced dissociation (HCD) favors the production of lower-m/z fragment ions. At 28 V, HCD allowed for the acquisition of accurate mass values for the smaller glycan fragment ions (m/z 427, 242, 204, and 186). For monosaccharides not producing clear oxonium ions, accurate mass was determined by calculating the accurate mass difference from the observed neutral loss (m/z 162 and 223). Plausible elemental formulae for each of the glycan fragments were determined using an Elemental Composition Calculator (http://www.wsearch.com.au/Tools/elemental_composition_calculator.htm) using the mean accurate mass values obtained from duplicate MS/MS runs, with a tolerance of 10 millimass units (mmu).

LPS purification, gel electrophoresis, and immunodetection. Glycine gel electrophoresis was performed using a 12.5% separating gel with a 4.5% stacking gel (29). Colonies were solubilized and incubated with 3.3 mg/ml proteinase K for 1 h at 60°C prior to loading on gels. For immunodetection, a murine monoclonal antibody to *F. tularensis* LVS lipopolysaccharide (LPS) O-side chain (ab2033) (Abcam, Cambridge, United Kingdom) was used. A horseradish peroxidase-labeled antibody (Amersham, United Kingdom) was used as a secondary antibody. The substrate 3,3′-diaminobenzidine tetrahydrochloride (DAB) was used as suggested by the Sigma Chemical Company until color developed.

Infection of mice with *F. tularensis* subsp. *tularensis* SchuS4 and Δ*FTT0791*::Cm and Δ*FTT0798* mutants. The bacteria were harvested after growth for 18 h at 37°C on BCGA agar. All procedures were carried out in accordance with Home Office guidelines. Groups of 10 or 6 adult female BALB/c mice (Charles River Laboratories) aged 6 to 8 weeks were infected with 0.1, 10^0, 10^1, and 10^2 CFU of each of the strains via the subcutaneous route and observed for 21 days. Humane endpoints were strictly observed, so that if an animal displayed irreversible signs of tularemia, it was promptly culled, thus avoiding undue distress. Irreversible signs include the following symptoms: unresponsive to extraneous stimuli and provocation, immobile, not self-righting, pronounced starring all over coat, and permanent pronounced hunching.

RESULTS

***F. tularensis* subsp. *tularensis* strain SchuS4 DsbA is reactive with glycostain.** Prokaryotes produce an array of unusual monosaccharides and glycan structures that are often difficult to characterize using the analytical technologies developed for the eukaryotic glycans and glycoproteins. Glycoreactive spots corresponding to two proteins were identified during this study: PilA and DsbA. Our studies focused on DsbA. Many discovery studies of bacterial glycoproteins commence with observation of aberrant protein migration on one-dimensional (1D) or two-dimensional (2D) polyacrylamide gels. Two-dimensional polyacrylamide gel electrophoresis (2D-PAGE) of whole bacterial cell lysate of *Francisella tularensis* subsp. *tularensis* strain SchuS4 showed that DsbA resolved into four proteins with different molecular masses and pIs (as indicated in Fig. 1A by black arrows). A duplicate 2D polyacrylamide gel was stained with Emerald Q glycostain (Fig. 1B). Only three of the four spots were glycoreactive. All four spots were identified as the hypothetical protein DsbA by nanoliquid chromatography coupled to tandem mass spectrometry analysis (nLC-MS/MS) of their tryptic digests (see next section). The three glycoreactive protein spots had observed molecular masses (pIs shown in the parentheses) of 47.0 kDa (4.55), 43.0 (4.65), and 41.5 (4.75). The single nonglycoreactive spot had an approximate molecular mass of 38.5 kDa (and a pI of 4.8), which is in close agreement with the predicted unmodified-protein molecular mass. Our experiments with Emerald Q glycostain showed that the glycostain reacted only with DsbA and PilA protein spots, and we did not observe any other glycoreactive proteins in our studies.

nLC-MS/MS analysis of *F. tularensis* subsp. *tularensis* DsbA peptide digests. The tryptic digests of the glycoreactive protein spots could be readily assigned to unmodified peptides within the DsbA protein sequence, thus proving the identities of the glycoreactive and unreactive spots. Several MS/MS spectra were derived from peptides that appeared to possess a glycan

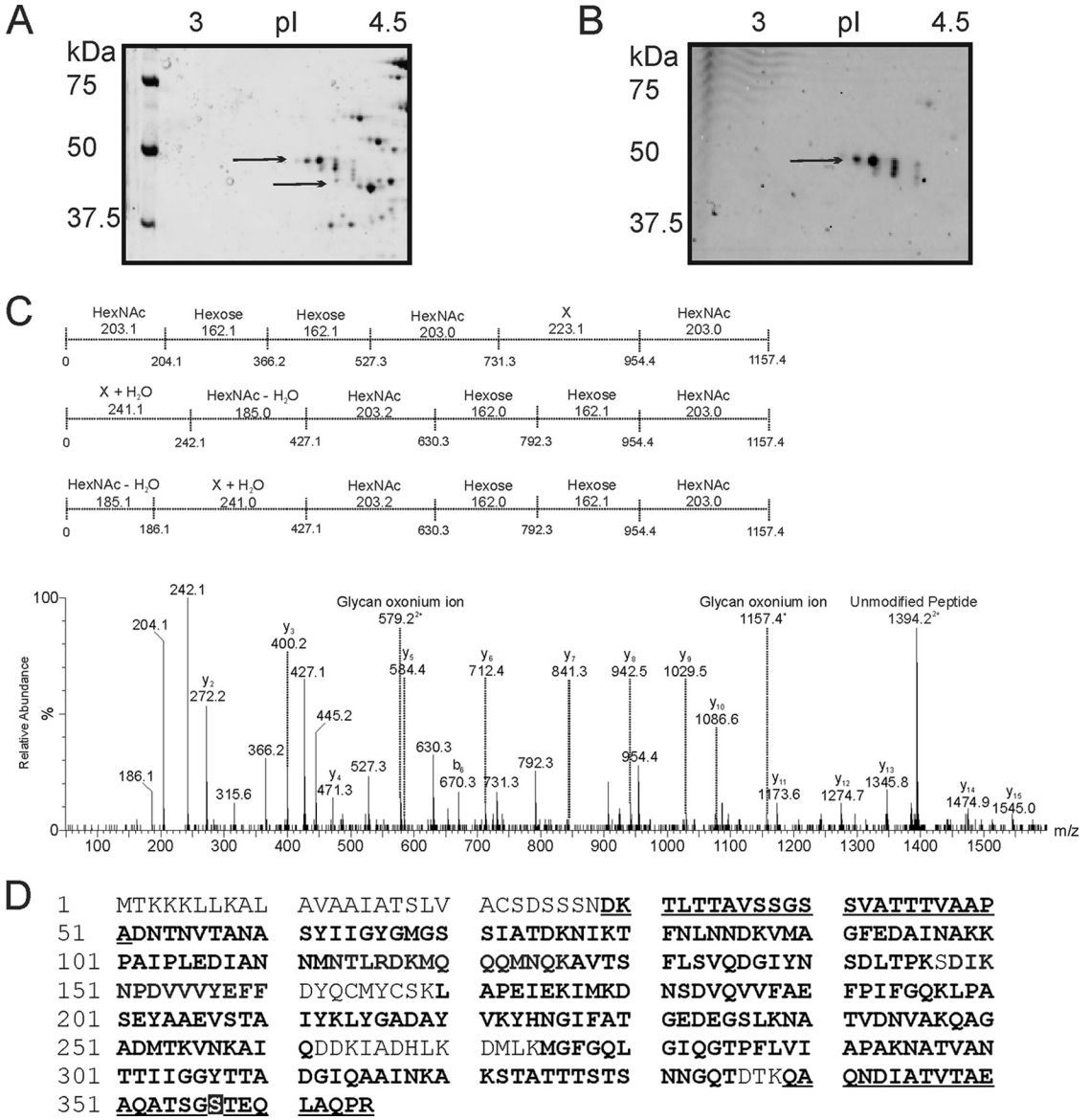

FIG. 1. (A and B) Zoom images of DsbA protein from *F. tularensis* subsp. *tularensis* strain SchuS4 resolved by 2D gel and tandem mass spectrometry analysis of the putative glycopeptide. The pI gradient is shown at the top of the gels, and the positions of molecular mass markers (in kilodaltons) are shown to the left of the gels. (A) *F. tularensis* subsp. *tularensis* strain SchuS4 stained with Sypro Ruby. Wild-type SchuS4 protein-stained image shows 4 protein spots that were identified by nLC-MSMS of their tryptic digests as DsbA. (B) *F. tularensis* subsp. *tularensis* strain SchuS4 stained with Emerald Q glycostain. The gel shows three predominant glycol-reactive protein spots, corresponding to DsbA. Proteins with different molecular masses and pIs in panels A and B are indicated by the black arrows. (C) nLC-MS/MS spectrum of the quadruply protonated $T^{343–365}$ glycopeptide at *m/z* 986.7. In the spectrum shown at the bottom of the panel, relative abundance is shown on the *y* axis, and *m/z* is shown on the *x* axis. The spectrum is dominated in the high-*m/z* region by a doubly protonated ion corresponding to the unmodified peptide. Peptide related y and b type fragment ions are indicated. The glycopeptide was 1.156 Da heavier than the unmodified peptide. A glycan-related oxonium ion was visible at *m/z* 1,157. In addition, a series of ions that did not correspond to peptide ions were clearly visible. These ions were characterized by a series of neutral losses from *m/z* 1,157, comprising six losses at 203, 162, 162, 203, 223, and 203 (in the order shown) and the same monosaccharides in the reverse orientation, 203, 223, 203, 162, 162, and 203. These masses could plausibly represent monosaccharides such as HexNAc (203) and hexose (162). The loss of 223 does not correspond to a known monosaccharide and is indicated as X in the figure. (D) Peptide sequence coverage obtained from MS/MS sequencing of DsbA digested with either trypsin or Asp-N. Sequenced peptides are indicated in bold type, and glycopeptides are shown in bold type and underlined. A glycopeptide, at the N-terminal region of the protein was identified: ^{29}DKTLTTAVSSGSSVATTTVAAPA^{51}. Another glycopeptide, ^{343}DIATVTAEAQATSGSTEQLAQ PR^{367}, the Asp-N fragment of tryptic digests, was detected in DsbA gel spots, and the mapped glycosylation site of the T^{32} glycopeptide is indicated in white-on-black type.

modification. Figure 1C shows the peptide MS/MS spectrum of the tryptic glycopeptide ^{343}QAQNDIATVTAEAQATSGSTE QLAQPR^{365}. Peptide type y and b ions were observed at low intensities, and the MS/MS spectrum was dominated by putative carbohydrate-related fragment ions at *m/z* 954, 792, 630, 427, and 204. A weaker ion at *m/z* 1,157 was thought to be the glycan oxonium ion. The total mass of the glycopeptide was 3,941.8 (predicted peptide mass of 2,785.6), suggesting a total

glycan mass of 1,156 Da. On the basis of this information and the deduced mass differences between putative glycan-related ions (indicated in Fig. 1C), the total sugar is comprised of monosaccharides with masses of 203, 223, 203, 162, 162, and 203 Da (monosaccharides in the total sugar in the order shown). Other glycan-related ions were observed at *m/z* 242, 324, 366, and 527 and were formed from fragmentation of the glycan, which suggests that the two isobaric glycopeptides were present, with the glycan attached to the peptide in the opposite orientation (monosaccharides with masses of 203, 162, 162, 203, 223, and 203 Da). In addition, oxonium ions from the monosaccharide components of the glycan were also observed at *m/z* 204 (putative *N*-acetylhexosamine) and 163 (putative hexose). Peptide sequence coverage obtained from MS/MS sequencing of DsbA digested with either trypsin or Asp-N and the sequenced peptides are indicated in Fig. 1D.

The ^{343}QAQNDIATVTAEAQATSGSTEQLAQPR^{365} peptide was also observed with a slightly different glycan modification. In the MS/MS spectrum of the triply charged ion at *m/z* 1,342.3, the doubly charged unmodified peptide ion was visible at *m/z* 1,393 and a putative glycan oxonium ion was visible at *m/z* 1,237.4 (data not shown). A neutral loss of 79.9, plausibly a phosphate group, from this oxonium ion yielded *m/z* 1,157. Further neutral losses from this oxonium ion were in the same sequence described above, suggesting the same monosaccharide composition with the addition of 80 Da. This mass could be attributed to phosphorylation likely of the terminal sugar monosaccharide.

Further identification of glycopeptides from MS/MS data of in-gel tryptic digests proved challenging. Some of the predicted tryptic peptides were greater than 20 amino acids in length and therefore difficult to sequence by nLC-MS/MS. A further set of gel spots were digested with the enzyme Asp-N, which cleaves on the N-terminal side of asparagine residues. Inspection of the resulting peptide MS/MS spectra revealed two putative glycopeptides, modified with a 1,156-Da glycan. The first peptide, ^{347}DIA TVTAEAQATSGSTEQLAQPR^{365}, was the Asp-N fragment of the glycopeptide detected in tryptic digests of DsbA gel spots. A second glycopeptide, this time at the N-terminal region of the protein, was identified: ^{29}DKTLTTAVSSGSSVATTTVAAPA^{51}. The MS/MS spectrum had a clear series of peptide y and b ions, in addition to a glycan oxonium ion at *m/z* 1,157. The glycan-related fragment ion described above was also visible (see Fig. S3 in the supplemental material). No further glycopeptides could be identified, and the total peptide sequence coverage is indicated in Fig. 1D.

Determination of glycan attachment sites. The native protein DsbA proved difficult to enrich from *F. tularensis* subsp. *tularensis* SchuS4 in quantities sufficient for glycoprotein characterization by multiple MS methods. We therefore used a recently developed approach based upon ion pairing normal-phase liquid chromatography (IP-NPLC) by the method of Ding et al. (12) to enrich the tryptic glycopeptide $T^{343–365}$ from a total tryptic proteome digest of *F. tularensis* subsp. *tularensis* SchuS4. The base peak chromatogram (BPC) of the SchuS4 total tryptic proteome digest showed two phases of separation; first, nonglycosylated peptides eluted, followed by glycopeptides as indicated (see Fig. S3a in the supplemental material). Glycopeptide-containing fractions were collected and analyzed by nLC-MS/MS and the tryptic glycopeptide. The DsbA glycopeptide ^{343}QAQNDIATVTAEAQATSGS TEQLAQPR^{365} was detected as the 3+ and 4+ ion, eluting at 16 min. This peptide was collected over sequential separations until sufficient glycopeptide material was accumulated for further MS studies (Fig. 2).

Electron transfer dissociation (ETD) has been shown to preserve posttranslational modification during peptide fragmentation and has proved useful in our past work, mapping *O*-linkage sites of flagellins. We therefore sought to map the glycan attachment site of the $T^{343–365}$ glycopeptide. ETD MS/MS was carried out, with fluoranthene as the anionic reagent. The resulting glycopeptide MS/MS spectrum, shown in Fig. 2A, was highly complex. Unusually, an intense glycan oxonium ion was visible (*m/z* 1,157), indicating the glycan modification to be highly labile under these conditions. Both doubly and singly charged peptide c and z ion series were observed. As indicated in Fig. 2A, the c, z, c plus glycan and z plus glycan ion series were observed. These ion series indicated that the glycan modification was at the C-terminal end of the peptide. Furthermore, the data suggested that serine 355 was modified through *O*-linkage, although definitive interpretation was difficult due to closely overlapping ion series. The peptide size, glycan size, and charge distribution on the peptide all made further attempts to optimize fragmentation by ETD difficult. Therefore, to unambiguously assign the site of *O*-linked attachment, purified glycopeptide was subjected to base-catalyzed hydrolysis in the presence of NH_4OH whereby the β-elimination product incorporated a newly formed amino group of a distinct mass (39). In this way, *O*-linked Ser and Thr residues yield modified amino acids of neutral masses of 86 and 100 Da, respectively. In this case, only Ser355 was modified, as evidenced by a mass shift of 86 Da between y11 and y12 (Fig. 2B).

Structural characterization of *O*-linked glycan moieties by MS/MS. Due to challenges in isolating glycopeptides in large quantities (attempts to overexpress the DsbA homologue in *F. tularensis* failed [data not shown]), we have not been able to isolate sufficient glycopeptide for nuclear magnetic resonance (NMR) structural studies that are required to determine the structure and absolute configuration of the hexasaccharide moiety. Instead, we have used high-resolution multistage MS analyses to provide information on the glycan structure composition. Inspection of the glycan fragmentation pattern of the *m/z* 1,157 oxonium ion within the DsbA glycopeptide MS/MS spectrum showed neutral losses corresponding to putative monosaccharides such as HexNAc and hexose, as described earlier. One neutral loss of 223 and a glycan-related fragment ion, *m/z* 242, could not be readily identified. Multistage mass spectrometry allows fragmentation of ions within an MS/MS spectrum. MS3 fragmentation of *m/z* 242 showed a neutral loss of water, yielding an ion of *m/z* 223 (Fig. 2C). A further loss of 18 from *m/z* 223 yielded *m/z* 205, an unidentified glycan fragment ion. A loss of *m/z* 98 from the parent ion likely corresponds to the loss of phosphate and water and yields the fragment ion at *m/z* 144.9.

MS4 analysis of the fragment ion at *m/z* 144.9 yielded a single daughter ion at *m/z* 116.9 (possible loss of CO). From these data, the *m/z* 242 sugar fragment ion corresponds to a 144-Da sugar, modified with a phosphoric acid.

Accurate mass measurements were performed wherever possible on glycan-related fragment ions in glycopeptide MS/MS spectra to determine the most plausible elemental formula for each monosaccharide moiety. The accurate masses

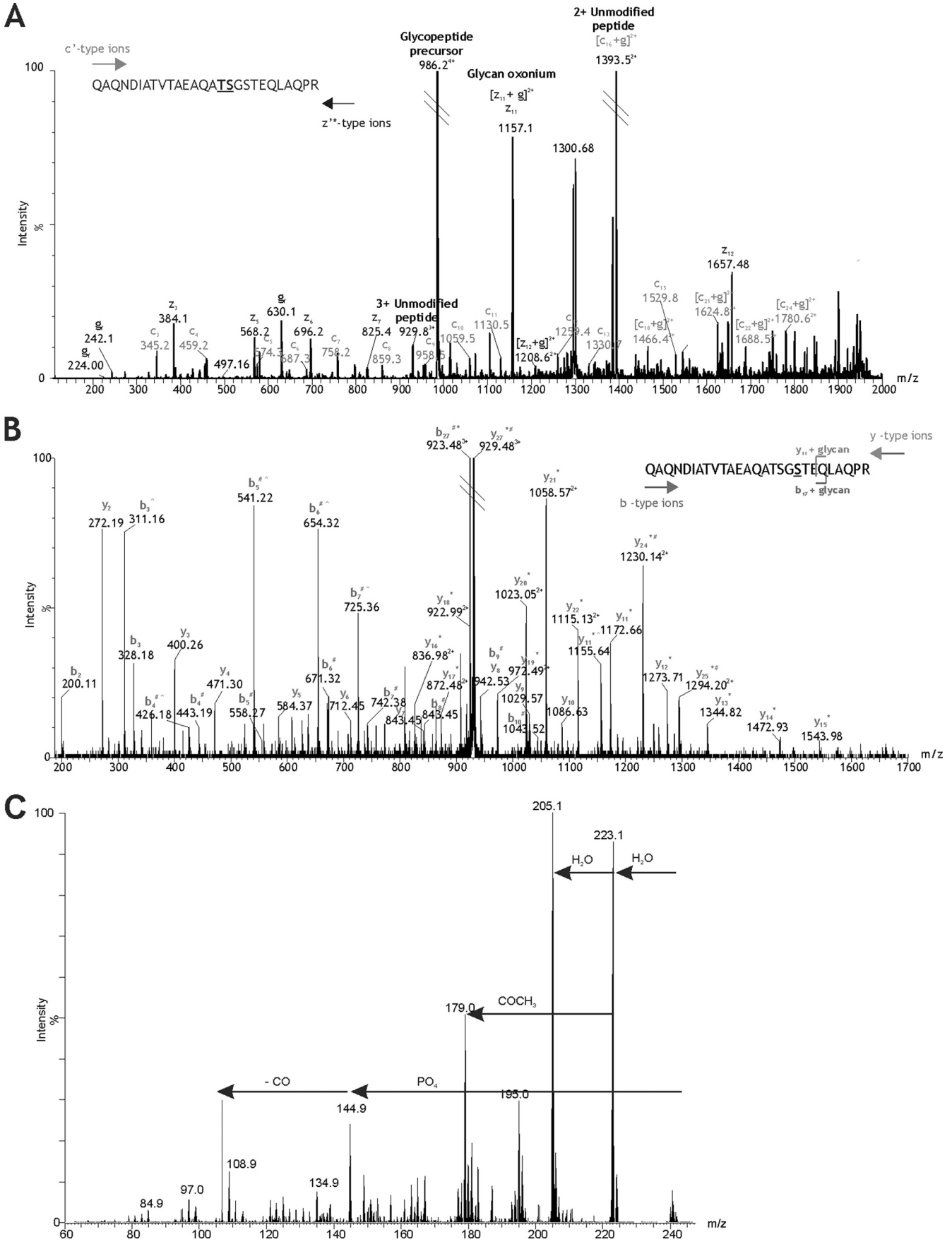
A
c'-type ions
QAQNDIATVTAEAQATSGSTEQLAQPR
z'*-type ions
Glycopeptide precursor
986.2^4+
Glycan oxonium
[z11 + g]^2+
z11
1157.1
2+ Unmodified peptide
[c16+g]^2+
1393.5^2+
1300.68
3+ Unmodified peptide
825.4
929.8^3+
1208.6^2+
1657.48
Intensity
%
m/z
B
y -type ions
QAQNDIATVTAEAQATSGSTEQLAQPR
b -type ions
y11 + glycan
b17 + glycan
923.48^3+
929.48^2+
1058.57^2+
541.22
654.32
272.19
311.16
725.36
1230.14^2+
1023.05^2+
922.99^2+
1115.13^2+
1172.66
1155.64
836.98^2+
872.48^2+
942.53
972.49^2+
1029.57
1086.63
1273.71
1294.20^2+
1344.82
1472.93
1543.98
400.26
328.18
200.11
471.30
671.32
584.37
712.45
742.38
843.45
426.18
443.19
558.27
1043.52
Intensity
%
m/z
C
205.1
223.1
H2O
H2O
COCH3
179.0
- CO
PO4
195.0
144.9
108.9
134.9
97.0
84.9

and top-ranked plausible elemental compositions are shown in Table S3 in the supplemental material. The top-ranked elemental formula of the ion of neutral loss of 162.1 Da indicated that this was a hexose sugar. A weak oxonium ion at *m/z* 163.1 was also observed. The neutral loss of 203.1 and the corresponding glycan oxonium at *m/z* 204.1 gave a top-ranked plausible elemental formula corresponding to a HexNAcHexNAc moiety. This was confirmed by the mass measurement of the commonly observed dehydrated HexNAc-related ion at *m/z* 186.1.

Interestingly, the top-ranked plausible elemental formulae of the glycan-related ion at *m/z* 242.1 supported our suggestion of a phosphate linkage within the sugar. This was also true for the neutral loss of 223 Da, corresponding to this unknown sugar. The accurate masses of other glycan-related fragment ions were also measured and are listed in Table S3 in the supplemental material, all corresponding to fragments of the complete hexose sugar. Overall, these data supported our suggestion that the modifying sugar is a hexasaccharide of composition HexNAc-unknown sugar (X)-HexNAc-hexose-hexose-HexNAc.

Production and characterization of defined *FTT0791*::Cm and *FTT0798* mutants of *F. tularensis* SchuS4. In order to begin to understand the role of glycosylation in virulence, we inactivated the *FTT0791* and *FTT0798* genes in *F. tularensis* subsp. *tularensis* SchuS4. The Δ*FTT0791*::Cm mutant was constructed by replacing 701 bp of the gene with an antibiotic resistance marker. The Δ*FTT0798* (putative glycosyltransferase gene) mutant had an in-frame deletion (start and stop codons separated by a BamHI site).

Southern blotting, PCR, and sequencing were used to identify double-crossover mutants which are referred to as the Δ*FTT0791*::Cm and Δ*FTT0798* mutants (see Fig. S1 in the supplemental material). RNA was isolated from both mutants, and reverse transcription-PCR (RT-PCR) was carried out to confirm the polarity of the mutants by looking for transcription of the downstream genes (see Fig. S2 in the supplemental material). Both mutants did not produce an amplicon after RT-PCR for their respective target genes, and furthermore, the Δ*FTT0791*::Cm mutant did not produce an amplicon for the *FTT0793* gene, and therefore, it was deemed a polar mutant.

Glycoproteomics of strain SchuS4 and Δ*FTT0791*::Cm and Δ*FTT0798* mutants. In order to determine whether the *FTT0789-FTT0800* cluster is involved in the biosynthesis of a glycoreactive moiety, we compared the 2D gel glycostain profiles of wild-type *F. tularensis*, an O-antigen gene cluster mutant (Δ*wbtDEF*::Cm) (53), and the Δ*FTT0798* and Δ*FTT0791*::Cm mutants. The DsbA protein was expressed by the wild type and all three mutants (as demonstrated by arrows in the Sypro Ruby staining of the protein in Fig. 1A and 3a, c, and e). The DsbA glycoforms were absent in the Δ*FTT0798* and Δ*FTT0791*::Cm mutants as demonstrated by Emerald Q staining in Fig. 3b and d, but in the O-antigen mutant, the glycoforms were present as shown in Fig. 3f. For the wild type, four DsbA protein spots were observed in the Sypro Ruby-stained gels, whereas only three of these spots reacted with Emerald Q glycostain (indicating three protein forms with glycan and one form with no glycan [Fig. 1A and B]). The O-antigen mutant, the Δ*wbtDEF*::Cm mutant, had the same glycoreactive profile as wild-type SchuS4 (Fig. 3e and f), indicating that this mutation had no effect upon potential posttranslational modification of DsbA. However, cell lysates of the Δ*FTT0791*::Cm and Δ*FTT0798* mutants showed no reactivity with glycostain (Fig. 3b and d). For the Δ*FTT0791*::Cm and Δ*FTT0798* mutants, the Sypro Ruby-stained single DsbA spots had a molecular mass and pI of 38.5 and ~4.8, respectively, which are in close agreement with the predicted molecular mass and pI of unmodified DsbA. In agreement with these observations, no glycopeptides or partial glycan chains were identified in tryptic digests of DsbA from these mutants by MS (see Fig. S4 in the supplemental material), making the function of the *FTT0791* and *FTT0798* genes difficult to elucidate.

FIG. 2. Mapping the modification site of DsbA $T^{343–365}$ glycopeptide. (A) ETD mass spectrum of the IP-NPLC-purified glycopeptide precursor ion at *m/z* 986.60^{4+}. Peptide c′ and z′* type ions are annotated. A modified amino acid can be detected in an ETD spectrum by a peak corresponding to a c′ or z′* ion plus the glycan mass. The additional mass of the glycan is then observed for each of the subsequent c′ and z′* ions. The glycan (g)-modifying peptide $T^{343–365}$ is 1,156.41 Da. A prominent peak at *m/z* 1,157.12 could represent $[z_{11} + g]^{2+}$ (*m/z* 1,156.78), indicating that serine 355 is the site of modification. However, this peak could also represent the predicted *m/z* of z_{11} (*m/z* 1,157.56) and the glycan oxonium ion (*m/z* 1,157.41). Since the resolution is insufficient to assign charge state, serine 355 cannot be unambiguously annotated as the site of glycosylation. Threonine 354 also cannot be unambiguously annotated as the site of glycosylation, despite a prominent ion at *m/z* 1,394.52, which may represent $[c_{16} + g]^{2+}$ (*m/z* 1,393.90) as well as the doubly charged unmodified peptide ion (*m/z* 1,393.68). The fact that these two amino acids are adjacent to one another further adds to the uncertainty because neither is able to provide additional evidence for modification of the residue next to it. In this case, ETD produces two candidate amino acid residues for the site of glycosylation: threonine 354 and serine 355. (B) nLC-MS/MS spectrum of the triply charged β-eliminated peptide ion at *m/z* 929.48 isolated by IP-NPLC separation. Peptide y and b type ions are indicated. Glycan removal by β-elimination with NH_4OH results in loss of 1 Da from the modified amino acid residue. An observed loss of 1 Da (*) from the predicted y_{11} peptide ion to the N-terminal y_{27} peptide ion indicates that serine 355 is the site of glycosylation. Deamidation of the sole asparagine residue in the peptide sequence results in a 1-Da addition (#) to the b_4 peptide ion, which is also observed for all subsequent b ions detected to the C-terminal b_{27} peptide ion. The loss of 1 Da due to β-elimination and the addition of 1 Da due to deamidation results in no net *m/z* difference between the predicted unmodified peptide precursor ion and the observed β-eliminated peptide precursor ion. The same is true for several peptide fragment ions at either end of the sequence that are subject to both β-elimination and deamidation. Additionally, a gas phase neutral loss of NH_3 (∧) from the side chain of glutamine 341 results in several prominent peaks in the mid-*m/z* region corresponding to b ions 3, 4, 5, 6, and 7 minus 17 Da. A gas phase neutral loss of 17 Da was also observed for the β-eliminated y_{11} peptide ion. (C) MS3 analysis of unknown monosaccharide *m/z* 242. From the MS/MS spectrum of the quadruply protonated $T^{343–365}$ glycopeptide at *m/z* 986.7, the glycan monosaccharide-related ion at *m/z* 242.1 was selected for MS3 analysis. The resulting spectrum is shown, with plausible losses of functional groups indicated. Sequential losses of water and a putative phosphate group resulted in a mass of 144.1. MS4 analysis of the fragment ion *m/z* 144.9 yielded a single daughter ion at *m/z* 116.9 (possible loss of CO) (data not shown).

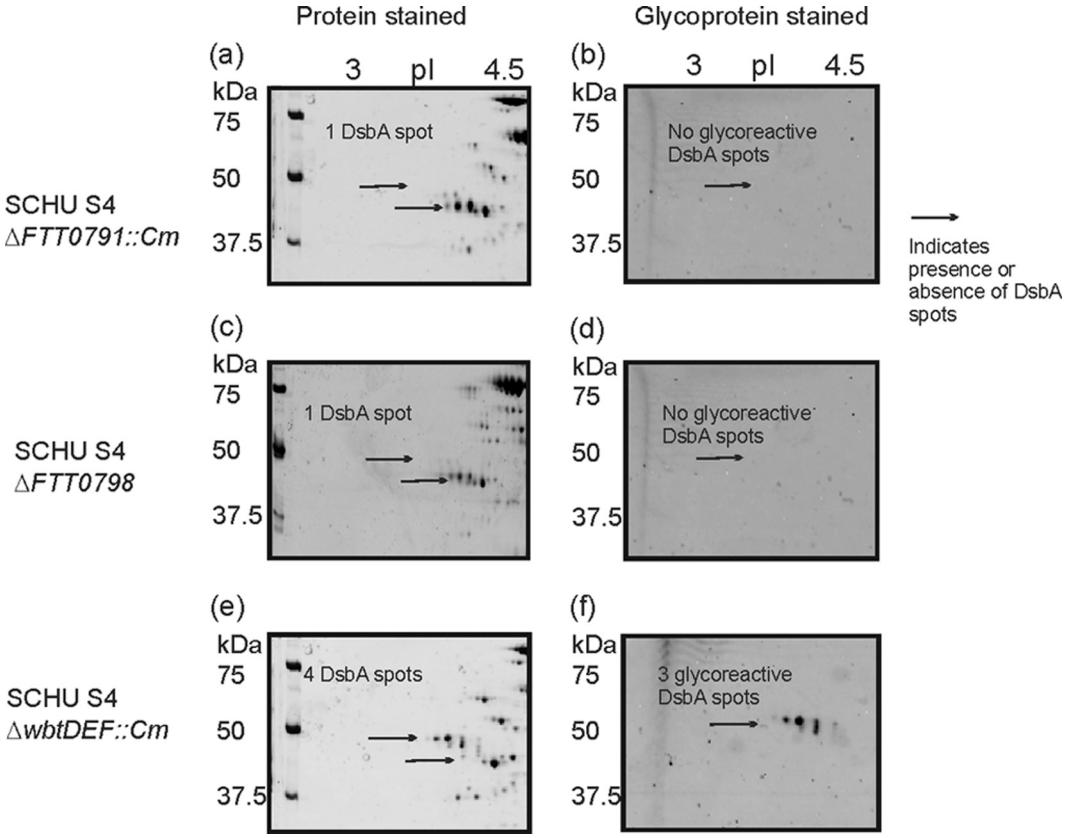

FIG. 3. 2D electrophoretic analysis of *F. tularensis* subsp. *tularensis* SchuS4 Δ*FTT0791*::Cm, Δ*FTT0798*, and Δ*wbtDEF*::Cm mutants. Zoom images of DsbA protein resolved by 2D-PAGE. Cell lysates (100 μg) were separated in the pH range 4 to 7. Each gel was stained sequentially with Emerald Q glycostain to visualize glycoreactive protein spots and then with Sypro Ruby protein stain. (a) SchuS4 Δ*FTT0791*::Cm mutant stained with Sypro Ruby; (b) SchuS4 Δ*FTT0791*::Cm mutant stained with Emerald Q glycostain; (c) SchuS4 Δ*FTT0798* mutant stained with Sypro Ruby; (d) SchuS4 Δ*FTT0798* mutant stained with Emerald Q glycostain; (e) SchuS4 Δ*wbtDEF*::Cm mutant stained with Sypro Ruby; (f) SchuS4 Δ*wbtDEF*::Cm mutant stained with Emerald Q glycostain.

To confirm that *FTT0798* and *FTT0791* were not involved in the biosynthesis of the O antigen, lipopolysaccharide (LPS) profiles of the Δ*FTT0791*::Cm and Δ*FTT0798* mutants were analyzed by Western blotting using a monoclonal antibody to *F. tularensis* subsp. *tularensis* LPS (Fig. 4). The monoclonal antibody reacted in similar manners with the wild-type strain and the two mutants. Although we have not observed the recently reported capsule (1), these data suggest that its production would be unaffected, as the O-antigen sugars are still produced in these mutants.

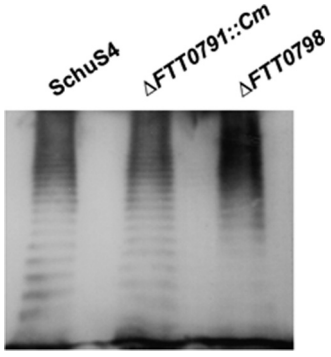

FIG. 4. LPS analysis of *F. tularensis* subsp. *tularensis* strain SchuS4 and Δ*FTT0791*::Cm and Δ*FTT0798* mutants. The membrane was probed with a monoclonal antibody (MAb) reactive with *F. tularensis* subsp. *tularensis* LPS. All strains have similar reactivities with the antibody.

Evaluation of the Δ*FTT0798* and Δ*FTT0791*::Cm mutants *in vivo*. The Δ*FTT0791*::Cm and Δ*FTT0798* cluster mutants cannot glycosylate DsbA, indicating that at least two of the genes of the *FTT0789-FTT0800* cluster play a role in biosynthesis of the glycan. Both mutants were used to investigate the possible role of the glycan *in vivo*. The virulence of Δ*FTT0798* and Δ*FTT0791*::Cm mutants of *F. tularensis* subsp. *tularensis* was compared to that of the wild-type strain SchuS4 in mice. Subcutaneous administration of 0.1, 10^0, 10^1, and 10^2 CFU was carried out for each strain, and mice were monitored for 21 days postchallenge. Humane endpoints were strictly observed, and animals deemed incapable of survival were humanely culled. Mice succumbed at similar times (day 6 or 7) at comparable doses (to wild type), indicating that the deletion of *FTT0791* and *FTT0798* had no effect on virulence under these conditions (Table 2). The median lethal dose (MLD) that induced morbidity or death was calculated by the method of Reed and Muench (40). For the wild-type strain, the MLD, by

TABLE 2. Infection and survival of BALB/c mice challenged with different doses of three *F. tularensis* subsp. *tularensis* strains

Challenge strain	Challenge dose (CFU)	Survivors (%)
SchuS4 (wild type)	550	0
	55	0
	5.5	0
	0.55	50
Δ*FTT0798* mutant	590	0
	59	0
	5.9	0
	0.59	50
Δ*FTT0791*::Cm mutant	100	0
	10	50
	1	80
	0.1	100

the subcutaneous route, has been reported as 1.5 CFU for *F. tularensis* subsp. *tularensis* (18). In this model, our studies showed the MLDs for all the strains used were in close agreement with this (MLDs of 6.65 CFU for the Δ*FTT0791*::Cm mutant, 0.59 CFU for the Δ*FTT0798* mutant, and 0.55 CFU for strain SchuS4).

DISCUSSION

The last decade has seen an increase in the number of studies reporting glycosylation of prokaryotic proteins. This has established this form of posttranslational modification as an integrated part of prokaryotic biology. In many cases, extensive structural characterizations of bacterial glycoproteins have been completed, but research on the biological significance and utility of these novel glycoconjugates is in its infancy. Recent reports have suggested that strains of *Francisella* elaborate glycoproteins (3, 41). Here we show that the putative disulfide isomerase protein and essential virulence factor, DsbA, is modified in *O*-linkage with a hexasaccharide moiety.

The detailed characterization of prokaryotic glycoproteins still presents numerous technical challenges, many of which stem from the novel sugars synthesized by bacteria and difficulties in isolating bacterial glycoproteins. A novel analytical method, ion pairing normal-phase liquid chromatography (IP-NPLC), was used to enrich glycopeptides from total proteome lysates, allowing sufficient material to be collected for detailed MS studies. However, the amount of material required for full structural characterization of the carbohydrate by NMR remains prohibitive, even with recent advances in the study of partially purified peptidyl glycan samples (56).

Protein homologues of DsbA were identified within the *F. tularensis* subsp. *holarctica* LVS (FTL1096) and *F. novicida* (FTN0771) genome sequences. We have found that DsbA is glycosylated in other *F. tularensis* subspecies. In *F. tularensis* subsp. *holarctica* (data not shown) and *F. novicida*, homologous regions of the proteins were modified with glycan (see Fig. S5 in the supplemental material). The peptide derived from strain LVS was modified with a hexasaccharide of 1,156 Da, with the masses and sequences of monosaccharides identical to those observed with type A *F. tularensis* subsp. *tularensis* SchuS4 (data not shown). In *F. novicida*, the peptide was modified with a putative glycan with a mass of 1,181.5 Da. Inspection of putative glycan-related fragment ions within the peptide MS/MS spectrum suggested a composition of 203, 203, 162, 162, 203, and 248 Da, where the 203-Da peak is a putative HexNAc and the 162-Da peak is a putative hexose (see Fig. S2 in the supplemental material). The monosaccharide with a mass of 248 Da is an unknown glycan moiety. Table 1 lists the genes in the *FTT0789-FTT0800* cluster and their homologues in the *F. tularensis* subsp. *holarctica* LVS strain and *F. novicida*. All the genes have homologues in *F. tularensis* subsp. *holarctica* LVS, whereas in *F. novicida*, four of the genes have no homologues (*FTT0794*, *FTT0795*, *FTT0796*, and *FTT0800*). The absence of these genes may account for the structural differences between the glycan of *F. novicida* and the glycan of the LVS strain of *F. tularensis* subsp. *holarctica* and the SchuS4 strain of *F. tularensis* subsp. *tularensis*.

Searching the *Francisella tularensis* subsp. *tularensis* strain SchuS4 genome sequence for potential polysaccharide biosynthetic genes revealed the O-antigen biosynthetic locus, and a second cluster of genes, *FTT0798-FTT0800*. Table 1 lists the genes within the *FTT0789-FT0800* cluster, their annotated function, homologues in other *F. tularensis* strains, and their nearest homologues in other bacterial species. The *FTT0789-FT0800* cluster contains three genes encoding proteins with homology to glycosyltransferases, a *galE* homologue, a gene encoding a putative transport protein, and three genes annotated as encoding hypothetical proteins. One of these putative glycosyltransferase proteins (FTT0799) shows limited homology to the capsular polysaccharide glycosyltransferase, WcbB, from *C. jejuni*. Of note, homologues of the genes within this cluster are found within *F. tularensis* subsp. *holarctica* strain LVS. However, *F. novicida* lacks homologues of the three hypothetical proteins FTT0794 to FTT0796. The proteins encoded by these genes contain conserved domains for methyltransferase (FTT0795) and phosphocholine metabolism (FTT0794 and FTT0796). The role of this gene cluster has not been confirmed experimentally. *F. tularensis* subsp. *tularensis* genome encodes two homologues of PilO, the glycosyltransferase which mediates the transfer of sugars to pilin subunits in *P. aeruginosa* (30). These homologues are not in the *FTT0789-FTT0800* cluster described here. One homologue, *FTT0905*, is annotated in the SCHU S4 database as being a type IV pilin glycosylation protein on the basis of its sequence similarity to the pilin-targeting *P. aeruginosa* PilO oligosaccharyltransferase. Deletion of this gene affected glycan modification of PilA (Mike Koomey, personal communication). The second PilO homologue, FTT1158c, is also annotated as a type IV pilus glycosylation protein. We have not identified a role for this protein.

We have constructed *FTT0791* and *FTT0798* mutants in this study. The use of chloramphenicol resistance as a marker for the construction of mutants is not allowed in the United States. However, subject to a local risk assessment and national approval by regulatory bodies, it can be used in *F. tularensis* in the United Kingdom. Disruption of *FTT0791* resulted in loss of detectable glycosylation by 2D-PAGE and MS (Fig. 3). However, it is possible that disruption of the *FTT0791* gene introduces a pleiotropic phenotype that could indirectly affect the biosynthesis of other polysaccharides. We sought to address

this by making an alternative mutant with a *FTT0798* mutation, encoding a putative glycosyltransferase, within the *FTT0789-FTT0800* cluster. As observed with the Δ*FTT0791*::Cm mutant, only unglycosylated DsbA was detected in extracts from the *FTT0798* mutant, indicating a potential role of the *FTT0789-FTT0800* cluster in glycan synthesis. The protein encoded by *FTT0791* shows sequence homology with UDP-galactose-4-epimerase (GalE) from other bacteria. However, there are additional *galE* homologues (*wbtC* and *wbtF*) in the O-antigen biosynthesis cluster in *F. tularensis*, suggesting possible redundancy of this function. GalE catalyzes interconversion of UDP-galactose to UDP-glucose, and in many bacteria, it plays a key role in lipopolysaccharide biosynthesis. The reported structure of *Francisella* O antigen lacks galactose moieties, and the LPS from either the *FTT0791* or *FTT0798* mutant was immunologically unaltered regarding monoclonal antibody recognition. Taken together, this indicates that these mutations do not affect O-antigen biosynthesis. The potential involvement of the *FTT0791* gene in protein glycosylation suggests that the hexasaccharide moieties are likely to be galactose. In other bacteria, mutation of the *galE* gene has been shown to affect protein glycosylation. For example, in *N. meningitidis*, disruption of *galE* results in lack of incorporation of galactose into the pilin *O*-linked trisaccharide (25) and in addition results in a truncated LPS (63). The observation that both mutations resulted in no detectable protein glycosylation by MS perhaps suggests that the glycan moiety is assembled and transferred *en bloc* to the protein.

Gene mutations of *galE* in other bacteria have been shown to modulate virulence. For example, there was an increase in serum sensitivity in a *galE* mutant of *N. meningitidis* (27, 60) and reduced virulence of a *galE* mutant of *Pasteurella multocida* in mice (15). However, in our study, the *FTT0791* and *FTT0798* mutants were not attenuated in a murine model of tularemia. In contrast, our studies indicate that the role of *FTT0791* in *F. novicida* may differ from that of *F. tularensis* subsp. *tularensis.* We created a marked *F. novicida FTT0791* mutant. This was used to challenge mice. Groups of 6 mice were challenged with 10^3 and 10^5 CFU of *F. novicida FTT0791*::Cm mutant. After 64 days, all the mice had survived, demonstrating that deletion of *FTT0791* plays a role in virulence of *F. novicida*.

The DsbA glycoprotein has been identified as an essential virulence factor of virulent type A *F. tularensis* (37), with potential roles in immune activation (51) and protein folding (49). DsbA is annotated within the SchuS4 genome as a hypothetical protein of unknown function. However, a search using the LipoP 1.0 server (Technical University of Denmark via ExPASY) strongly suggests that it is a lipoprotein, with the signal sequence cleaved after residue A21 and lipoylation of residue C22. The DsbA protein is therefore expected to be periplasmic and is enriched in crude membrane proteome fractions (54). The protein has also been observed to migrate to multiple protein spots in bacteria recovered from murine spleen, suggestive of glycosylation in the infected host (55). Fold recognition (Phyre, Pfam, and FUGUE) suggests that there is a central core of the protein that belongs to the DsbA-like thioredoxin family (Com-1-like subfamily). This indicates a likely function in redox chemistry, confirmed by a recent study (49). This core domain includes residues 155 to 290. At the N terminus of the protein, another domain is detected covering residues 37 to 127 (Pfam): this is a domain that is commonly found N terminal to FKBP proteins: this is a dimerization domain. In other bacterial systems, disulfide bond formation is catalyzed primarily by the DsbA/DsbB system (26). In other bacteria, mutants lacking DsbA or DsbB exhibit pleiotropic phenotypes. Decreased motility stemming from improper flagellin formation has also been reported (11). Other virulence factors such as pili, toxins, and type III secretion systems can also be impacted because of the requirement for disulfide bond formation for protein functionality (13, 20, 24, 34, 35, 64). It is interesting to note that in the human pathogen *N. gonorrhoeae*, the DsbA protein is also glycosylated via *O*-linkage (59). In addition, the study demonstrated that numerous proteins, including PilE2, undergo *O*-linked glycosylation by the same glycan biosynthetic pathway. The *F. tularensis* subsp. *tularensis* PilA is not modified by a glycan in the *FTT0791* and *FTT0798* mutants (Mike Koomey, personal communication), suggesting a similar mechanism of glycosylation of PilA and DsbA in *F. tularensis*. Deletion of the *dsbA* homologous gene in the live vaccine strain (*F. tularensis* subsp. *holarctica* LVS) resulted in the accumulation of several proteins, speculated to be substrates for the enzymatic activity of DsbA (49). The majority of these proteins were annotated as hypothetical proteins with no close homologues, making interpretation of the role of DsbA challenging.

This is the first report confirming *O*-linked glycosylation of DsbA in *F. tularensis* and a role of genes in the *FTT0789-FTT0800* gene cluster. *F. tularensis* possesses at least two proteins that are modified with a glycan by *O*-linkage. We have demonstrated that the *FTT0791* and *FTT0798* genes are involved in DsbA glycosylation. The exact role that the glycan plays is still unclear. Our studies indicate that the glycan is not essential for virulence *in vivo* in the murine model of tularemia upon subcutaneous injection (an infection route that is similar to the natural infection route from ticks). Future studies will be focused on elucidation of the role of the glycan in the intracellular lifestyle of *F. tularensis*.

ACKNOWLEDGMENTS

This work was funded in part by the National Research Council Canada.

We thank Donna Ford, Ronda Griffiths, Michelle Nelson, Isobel Norville, and Helen Sharps for technical assistance. We acknowledge Simon Foote for help with bioinformatics analyses. We thank Michael Koomey and Wolfgang Egge-Jacbosen for critical reading of the manuscript.

REFERENCES

1. **Apicella, M. A., et al.** 2010. Identification, characterization and immunogenicity of an O-antigen capsular polysaccharide of *Francisella tularensis*. PLoS One **5:**e11060.
2. **Apweiler, R., H. Hermjakob, and N. Sharon.** 1999. On the frequency of protein glycosylation, as deduced from analysis of the SWISS-PROT database. Biochim. Biophys. Acta **1473:**4–8.
3. **Balonova, L., et al.** 2010. Multimethodological approach to identification of glycoproteins from the proteome of *Francisella tularensis*, an intracellular microorganism. J. Proteome Res. **9:**1995–2005.
4. **Banerjee, A., and S. K. Ghosh.** 2003. The role of pilin glycan in neisserial pathogenesis. Mol. Cell. Biochem. **253:**179–190.
5. **Bertani, G.** 1951. Studies on lysogenesis. I. The mode of phage liberation by lysogenic *Escherichia coli.* J. Bacteriol. **62:**293–300.
6. **Castric, P., F. J. Cassels, and R. W. Carlson.** 2001. Structural characterization of the *Pseudomonas aeruginosa* 1244 pilin glycan. J. Biol. Chem. **276:** 26479–26485.
7. **Chaban, B., S. Voisin, J. Kelly, S. M. Logan, and K. F. Jarrell.** 2006.

Identification of genes involved in the biosynthesis and attachment of *Methanococcus voltae* N-linked glycans: insight into N-linked glycosylation pathways in Archaea. Mol. Microbiol. **61:**259–268.
8. **Chamberlain, R. E.** 1965. Evaluation of live tularemia vaccine prepared in a chemically defined medium. Appl. Microbiol. **13:**232–235.
9. **Clackson, T., D. Gussow, and P. T. Jones.** 1991. PCR: a practical approach, p. 187–214. *In* M. J. McPherson, P. Quirke, and G. R. Taylor (ed.), PCR: a practical approach. Oxford University Press, Oxford, United Kingdom.
10. **Comstock, L.** 2009. Importance of glycans to the host-Bacteroides mutualism in the mammalian intestine. Cell Host Microbe **5:**522–526.
11. **Dailey, F. E., and H. C. Berg.** 1993. Mutants in disulfide bond formation that disrupt flagellar assembly in *Escherichia coli*. Proc. Natl. Acad. Sci. U. S. A. **90:**1043–1047.
12. **Ding, W., H. Nothaft, C. M. Szymanski, and J. Kelly.** 2009. Identification and quantification of glycoproteins using ion-pairing normal-phase liquid chromatography and mass spectrometry. Mol. Cell. Proteomics **8:**2170–2185.
13. **Ellermeier, C. D., and J. M. Slauch.** 2004. RtsA coordinately regulates DsbA and the *Salmonella* pathogenicity island 1 type III secretion system. J. Bacteriol. **186:**68–79.
14. **Ellis, J., P. C. F. Oyston, M. Green, and R. W. Titball.** 2002. Tularemia. Clin. Microbiol. Rev. **15:**631–646.
15. **Fernández de Henestrosa, A. R., et al.** 1997. Importance of the galE gene on the virulence of *Pasteurella multocida*. FEMS Microbiol. Lett. **154:**311–316.
16. **Forslund, A. L., et al.** 2006. Direct repeat-mediated deletion of a type IV pilin gene results in major virulence attenuation of *Francisella tularensis*. Mol. Microbiol. **59:**1818–1830.
17. **Golovliov, I., A. Sjostedt, A. Mokrievich, and V. Pavlov.** 2003. A method for allelic replacement in *Francisella tularensis*. FEMS Microbiol. Lett. **222:**273–280.
18. **Green, M., G. Choules, D. Rogers, and R. W. Titball.** 2005. Efficacy of the live attenuated *Francisella tularensis* vaccine (LVS) in a murine model of disease. Vaccine **23:**2680–2686.
19. **Guerry, P., et al.** 2006. Changes in flagellin glycosylation affect *Campylobacter* autoagglutination and virulence. Mol. Microbiol. **60:**299–311.
20. **Ha, U. H., Y. P. Wang, and S. G. Jin.** 2003. DsbA of *Pseudomonas aeruginosa* is essential for multiple virulence factors. Infect. Immun. **71:**1590–1595.
21. **Hamadeh, R. M., M. M. Estabrook, P. Zhou, G. A. Jarvis, and J. M. Griffiss.** 1995. Anti-Gal binds to pili of *Neisseria meningitidis*: the immunoglobulin A isotype blocks complement-mediated killing. Infect. Immun. **63:**4900–4906.
22. **Hegge, F. T., et al.** 2004. Unique modifications with phosphocholine and phosphoethanolamine define alternate antigenic forms of *Neisseria gonorrhoeae* type IV pili. Proc. Natl. Acad. Sci. U. S. A. **101:**10798–10803.
23. **Hollis, D. G., et al.** 1989. *Francisella philomiragia* comb. nov. (formerly *Yersinia philomiragia*) and *Francisella tularensis* biogroup *novicida* (formerly *Francisella novicida*) associated with human disease. J. Clin. Microbiol. **27:**1601–1608.
24. **Jackson, M. W., and G. V. Plano.** 1999. DsbA is required for stable expression of outer membrane protein YscC and for efficient Yop secretion in *Yersinia pestis*. J. Bacteriol. **181:**5126–5130.
25. **Jennings, M. P., et al.** 1998. Identification of a novel gene involved in pilin glycosylation in *Neisseria meningitidis*. Mol. Microbiol. **29:**975–984.
26. **Kadokura, H., F. Katzen, and J. Beckwith.** 2003. Protein disulfide bond formation in prokaryotes. Annu. Rev. Biochem. **72:**111–135.
27. **Kahler, C. M., et al.** 1998. The (α2→8)-linked polysialic acid capsule and lipooligosaccharide structure both contribute to the ability of serogroup B *Neisseria meningitidis* to resist the bactericidal activity of normal human serum. Infect. Immun. **66:**5939–5947.
28. **Kraemer, P. S., et al.** 2009. Genome-wide screen in *Francisella novicida* for genes required for pulmonary and systemic infection in mice. Infect. Immun. **77:**232–244.
29. **Laemmli, U. K.** 1970. Cleavage of structural proteins during the assembly of the head of bacteriophage T4. Nature **227:**680–685.
30. **Larsson, P., et al.** 2005. The complete genome sequence of *Francisella tularensis*, the causative agent of tularemia. Nat. Genet. **37:**153–159.
31. **Logan, S. M.** 2006. Flagellar glycosylation: a new component of the motility repertoire? Microbiology **152:**1249–1262.
32. **Mescher, M. F., and J. L. Strominger.** 1976. Purification and characterization of a prokaryotic glycoprotein from cell envelope of *Halobacterium salinarium*. J. Biol. Chem. **251:**2005–2014.
33. **Messner, P.** 2004. Prokaryotic glycoproteins: unexplored but important. J. Bacteriol. **186:**2517–2519.
34. **Miki, T., N. Okada, and H. Danbara.** 2004. Two periplasmic disulfide oxidoreductases, DsbA and SrgA, target outer membrane protein SpiA, a component of the *Salmonella* pathogenicity island 2 type III secretion system. J. Biol. Chem. **279:**34631–34642.
35. **Peek, J. A., and R. K. Taylor.** 1992. Characterization of a periplasmic thiol-disulfide interchange protein required for the functional maturation of secreted virulence factors of *Vibrio cholerae*. Proc. Natl. Acad. Sci. U. S. A. **89:**6210–6214.
36. **Prior, J. L., et al.** 2003. Characterization of the O antigen gene cluster and structural analysis of the O antigen of *Francisella tularensis* subsp. *tularensis.* J. Med. Microbiol. **52:**845–851.
37. **Qin, A. P., D. W. Scott, J. A. Thompson, and B. J. Mann.** 2009. Identification of an essential *Francisella tularensis* subsp. *tularensis* virulence factor. Infect. Immun. **77:**152–161.
38. **Quarry, J. E., et al.** 2007. A *Francisella tularensis* subspecies *novicida purF* mutant, but not a *purA* mutant, induces protective immunity to tularemia in mice. Vaccine **25:**2011–2018.
39. **Rademaker, G. J., et al.** 1998. Mass spectrometric determination of the sites of O-glycan attachment with low picomolar sensitivity. Anal. Biochem. **257:**149–160.
40. **Reed, L. J., and H. Muench.** 1938. A simple method for estimating fifty percent endpoints. Am. J. Hyg. **27:**493–497.
41. **Salomonsson, E., et al.** 2009. Functional analyses of pilin-like proteins from *Francisella tularensis*: complementation of type IV pilus phenotypes in *Neisseria gonorrhoeae*. Microbiology **155:**2546–2559.
42. **Schirm, M., et al.** 2004. Structural and genetic characterization of glycosylation of type a flagellin in *Pseudomonas aeruginosa*. J. Bacteriol. **186:**2523–2531.
43. **Schirm, M., et al.** 2004. Flagellin from *Listeria monocytogenes* is glycosylated with β-O-linked *N*-acetylglucosamine. J. Bacteriol. **186:**6721–6727.
44. **Schirm, M., I. C. Schoenhofen, S. M. Logan, K. C. Waldron, and P. Thibault.** 2005. Identification of unusual bacterial glycosylation by tandem mass spectrometry analyses of intact proteins. Anal. Chem. **77:**7774–7782.
45. **Schirm, M., et al.** 2003. Structural, genetic and functional characterization of the flagellin glycosylation process in *Helicobacter pylori*. Mol. Microbiol. **48:**1579–1592.
46. **Schmidt, M. A., L. W. Riley, and I. Benz.** 2003. Sweet new world: glycoproteins in bacterial pathogens. Trends Microbiol. **11:**554–561.
47. **Simon, R., U. B. Priefer, and A. Pühler.** 1983. A broad host range mobilisation system for *in vitro* genetic engineering: transposon mutagenesis in Gram negative bacteria. Biotechnology **1:**784–791.
48. **Stimson, E., et al.** 1995. Meningococcal pilin: a glycoprotein substituted with digalactosyl 2,4-diacetamido-2,4,6-trideoxyhexose. Mol. Microbiol. **17:**1201–1214.
49. **Straskova, A., et al.** 2009. Proteome analysis of an attenuated *Francisella tularensis* dsbA mutant: identification of potential DsbA substrate proteins. J. Proteome Res. **8:**5336–5346.
50. **Szymanski, C. M., S. M. Logan, D. Linton, and B. W. Wren.** 2003. *Campylobacter*: a tale of two protein glycosylation systems. Trends Microbiol. **11:**233–238.
51. **Thakran, S., et al.** 2008. Identification of *Francisella tularensis* lipoproteins that stimulate the Toll-like receptor (TLR)2/TLR1 heterodimer. J. Biol. Chem. **283:**3751–3760.
52. **Thibault, P., et al.** 2001. Identification of the carbohydrate moieties and glycosylation motifs in *Campylobacter jejuni* flagellin. J. Biol. Chem. **276:**34862–34870.
53. **Thomas, R. M., et al.** 2007. The immunologically distinct O antigens from *Francisella tularensis* subsp. *tularensis* and *Francisella novicida* are both virulence determinants and protective antigens. Infect. Immun. **75:**371–378.
54. **Twine, S. M., et al.** 2005. *Francisella tularensis* proteome: low levels of ASB-14 facilitate the visualization of membrane proteins in total protein extracts. J. Proteome Res. **4:**1848–1854.
55. **Twine, S. M., et al.** 2006. *In vivo* proteomic analysis of the intracellular bacterial pathogen, *Francisella tularensis*, isolated from mouse spleen. Biochem. Biophys. Res. Commun. **345:**1621–1633.
56. **Twine, S. M., et al.** 2008. Flagellar glycosylation in *Clostridium botulinum*. FEBS J. **275:**4428–4444.
57. **Twine, S. M., et al.** 2009. Motility and flagellar glycosylation in *Clostridium difficile*. J. Bacteriol. **191:**7050–7062.
58. **Verma, A., et al.** 2006. Glycosylation of b-type flagellin of *Pseudomonas aeruginosa*: structural and genetic basis. J. Bacteriol. **188:**4395–4403.
59. **Vik, A., et al.** 2009. Broad spectrum O-linked protein glycosylation in the human pathogen *Neisseria gonorrhoeae*. Proc. Natl. Acad. Sci. U. S. A. **106:**4447–4452.
60. **Vogel, U., H. Claus, G. Heinze, and M. Frosch.** 1997. Functional characterization of an isogenic meningococcal alpha-2,3-sialyltransferase mutant: the role of lipooligosaccharide sialylation for serum resistance in serogroup B meningococci. Med. Microbiol. Immunol. **186:**159–166.
61. **Voisin, S., et al.** 2005. Identification and characterization of the unique N-linked glycan common to the flagellins and S-layer glycoprotein of *Methanococcus voltae*. J. Biol. Chem. **280:**16586–16593.
62. **Voisin, S., et al.** 2007. Glycosylation of *Pseudomonas aeruginosa* strain Pa5196 type IV pilins with mycobacterium-like alpha-1,5-linked D-Araf oligosaccharides. J. Bacteriol. **189:**151–159.
63. **Wakarchuk, W., A. Martin, M. P. Jennings, E. R. Moxon, and J. C. Richards.** 1996. Functional relationships of the genetic locus encoding the glycosyltransferase enzymes involved in expression of the lacto-N-neotetraose terminal lipopolysaccharide structure in *Neisseria meningitidis*. J. Biol. Chem. **271:**19166–19173.
64. **Watarai, M., T. Tobe, M. Yoshikawa, and C. Sasakawa.** 1995. Disulfide oxidoreductase activity of *Shigella flexneri* is required for release of Ipa proteins and invasion of epithelial cells. Proc. Natl. Acad. Sci. U. S. A. **92:**4927–4931.
65. **Weiss, D. S., et al.** 2007. *In vivo* negative selection screen identifies genes required for *Francisella* virulence. Proc. Natl. Acad. Sci. U. S. A. **104:**6037–6042.